University of Sistan and Baluchestan

Chemical Process Design

Available online at http://cpd.usb.ac.ir/

Using Response Surface Methodology (RSM) to Evaluate the Drag Reduction by Polyacrylamide, Experimental and Statistical Investigation

Behrouz Raei

Department of Chemical Engineering, Mahshahr Branch, Islamic Azad University, Mahshahr, Iran. E-mail: behrouz.raei@iau.ac.ir

ARTICLE INFO

Article type:
Research Article

Article history:
Received: 2025-03-06
Received in revised form: 2025-04-12
Accepted: 2025-04-15
Published online: 2025-04-15

Keywords: *Polyacrylamide; Response Surface Methodology; Drag reduction; Friction factor*

ABSTRACT

In the present study, the effect of polyacrylamide (PAM) addition as a drag reducing agent on the hydraulic performance of water flow inside horizontal smooth circular pipe was investigated experimentally and statistically. Several experiments were performed under various operating circumstances such as fluid flow rates (Q) at the 6,8,10 L/min, concentrations (C) of 10,100, 200 ppm, and temperatures (T) of 30, 40, and 50°C. The main aim of this study was to establish the correlation between Darcy friction factor (f) and C, Q and T using response surface methodology (RSM). Different models were evaluated based on a series of quality indicators and charts. Some of the indicators that were investigated in this study include standard deviation (Std. Dev.), coefficient of determination (R2) and coefficient of variation (C.V). After checking the quality indicators and charts for different models, the quadratic model was selected as the optimal model. The values of Std. Dev, R2 and C.V for the quadratic model were 0.0011, 0.9856, and 3.18%, respectively. The most optimum f is 0.022. At a temperature of 30°C, this condition was achieved in samples at C=182.111 ppm and Q = 10 L/min.

Cite this article: Raei, B., (2025), Using Response Surface Methodology (RSM) to Evaluate the Drag Reduction by Polyacrylamide, Experimental and Statistical Investigation, *Chemical Process Design*, 4(1), 44-59. http//doi.org/10.22111/cpd.2025.51346.1051

DOI: http//doi.org/10.22111/cpd.2025.51346.1051

Publisher: University of Sistan and Baluchestan.

1. Introduction

Adding a minor quantity of high molecular weight polymer in a fluid can significantly decrease frictional drag in turbulent flows within pipes or ducts. This phenomenon, referred to as friction reduction, was initially documented by Toms in 1948 [1]. After then, friction reduction has received increasing attention as it has become widely used in industry. Polymer additives are useful in a diversity of usages, containing very long-distance transportation of liquids, firefighting processes and domestic plumbing. To gain a deeper insight into the observed phenomenon, several

investigations have been operated regarding the reduction in resistance attributed to the polymer in turbulent flow. The first empirical investigations on this topic were conducted by Toms [1] and Virk [2]. Virk demonstrated notable differences in the behavior of polymers under laminar and turbulent flows. Although no reduction in friction was monitored in laminar flows, a remarkable reduction was achieved in turbulent flow. He was the pioneer in demonstrating that a maximum limit for friction reduction exists, which is not influenced by both the diameter of the pipe and the type of polymer used in turbulent pipe flow; this limit is known as the Virk asymptote. Several investigations indicate that the ability of polymers to reduce friction in turbulent flow significantly influenced by several factors, including the molecular weight (Mw), type and concentration of the polymer, the polymer degradation, the preparation type of the solutions, the solvent characteristics, the solution temperature and etc. [3]. Following the initial observations regarding friction reducing polymers, numerous examinations have been conducted in this field.

Kim et al. [4] examined the influence of concentration (1, 5, 10, and 20 ppm) and molecular weight (Mw) of polyethylene oxide (PEO) as a drag reducing agent (DRA). A maximum drag reduction of 50% was recorded at a concentration of 20 ppm and an Mw of 4×10^6. They also declared that the rate of drag reduction improved as the Reynolds number (Re) and the Mw of the DRA increased. Raei and Peyghambarzadeh [5] conducted an experimental investigation on drag reduction. The study involved a comparison of the efficiency of three biological macromolecules, namely xanthan gum (XG), carboxymethyl cellulose (CMC), and guar gum (GG), alongside three synthetic macromolecules, which included polyacrylic acid (PAA), PEO, and PAM. They showed that all drag reduction (DR%) were increased by polymers except GG. Increasing the fluid flow rate resulted in a decline in DR% for nearly all macromolecules. Sung et al. [6] compared PAM and PEO polymers under various working conditions, ultimately determining that PAM exhibits higher shear resistance compared to PEO. This macromolecule has been suggested as a superb additive for applications involving long-period transportation.

From very recent research, references [7-14] can be mentioned. Various investigations have been conducted on the drag reduction properties of PAM in different devices, which have sometimes reported contradictory results. On the other hand, some studies [15, 16] have stated that due to the high mechanical strength of PAM chains, their DR does not decrease over time compared to other macromolecules. Thus, PAM has been selected in preference to other polymers for the current research. Table 1 presents a summary of various studies conducted on DR using PAM under different operating conditions. As displayed in Table 1, the maximum DR% of PAM was viewed by Sitaramaiah & Smith [17] and Jouenne et al. [18] by 80% while the minimum DR% was gained by Raei et al. [19] that was negligible. A compilation of review articles concerning the DR of polymer solutions can be found in references [20-26]. One significant challenge associated with the usage of polymers in friction reduction applications is the degradation of these polymers. This problem is the result of high shear stress in turbulent flow, which can lead to important damage to the polymer's ability to reduce friction. References [3, 27-33] have studied the mechanical degradation of polymers. Although numerous studies have been conducted on the DR, but its concept remains not entirely comprehended. As stated by Virk et al. [34], DR follows two mechanisms depending on the type of polymer: in the first mechanism, polymers remain coiled at rest. These polymers necessitate a specific degree of turbulence to stretch and subsequently begin to decrease drag. In the second mechanism, the polymers remain in an extended state when at rest. In other words, if the second mechanism is prevailing, DR is expected to be initiated more rapidly. The mechanism of DR for PAM solutions is evidently categorized as the second mechanism. The viscoelastic characteristics are more efficient

in decreasing turbulence than the viscous force generated in the fluid [35] , and linearization of the structure of the coiled molecules is an efficient element in DR although investigations have exhibited that elastic effects could decrease drag [35, 36].

Few studies have been done to provide equations to predict the friction factor of DRA. Also, rarely has statistical analysis been done in the field of DR. Ozmen and Boersma [37] have introduced an empirical equation to estimate the Darcy friction factor as a function of Reynolds number and polymer concentration for PAM in turbulent flow. Cheng et al.[38] have investigated statistically the drag reduction property of a premixed slurry drag reducer using RSM. Using the Taguchi method, Raei [39] has studied statistically the drag reduction property of polyacrylonitrile (PAN) in circular pipes.

Table 1. Comparison of using PAM as a DRA in single phase flow in previous experimental studies

Reference	Base fluid	Experimental system	Operating conditions	Max DR%
Varnaseri et al. [40]	Distilled water	Compact heat exchanger	Re: 200 −1400 C: 0 –150 ppm	14
Sung et al. [6]	Distilled water	Rotating disk apparatus	N_{Re} >3×10^5 C: 10 −50 ppm	29
Sitaramaiah and Smith [17]	Distilled water	Pipe flow	Q: 0.45–4.3 m^3/h C: 100–1000 ppm	80
Sandoval et al. [41]	Filtered water	Pipe flow	Re: 85,000–110,000 C: 25–200 ppm	70
Raei et al. [19]	Water	Double tube heat exchanger	Re: 18,000 – 40,000 C: 0 –100 ppm	Negligible
Pereira et al. [15]	Water	Axial symmetric double gap geometry	Re: max 1360 C: max 37.5 ppm	22
Lim & Choi [42]	Water	Rotating disk apparatus	N_{Re} >3×10^5 C: 1.35 ppm	16
Liberatore et al. [43]	Tap water	Rectangular flow channel having a flat wall and a wavy wall	Re: 48,000 C: 200–1000 ppm	58
Khadom & Abdul-Hadi [44]	Crude oil	Pipelines	Re: 6,064–36,388 C: 10–50 ppm	40.64
Jouenne et al. [18]	Water	Pipelines	Re: max 561,438 C: max 2,000 ppm	80
Andrade et al. [45]	Water	Rotating cylindrical double gap device	Re: 1,360, 1,570 C: 50 ppm	24
Varnaseri and Peyghambarzadeh [46]	Distilled water	Pipelines	Q=0.5-20 L/min C: 10–150 ppm	50
Liu et al.[47]	Water	Two-dimensional (2D) channel	Re: 4000, 60,000 C: 60 ppm	50.15
Varnaseri and Peyghambarzadeh [48]	Distilled water	Finned tube heat exchanger	Re: 650, 1,500 C: 0 –100 ppm	12
Rho et al. [49]	Distilled water	Pipe flow	Re: 15,000- 35,000 C: 200 ppm	60
Den Toonder et al.[3]	Water	Pipe flow	Re: 12,400- 19,500 C: 20 ppm	61
Karami et al. [33]	Tab water& Deionized water	Pipe flow	Re: 18,280 C: 10 –50 ppm	60
Sandoval et al. [16]	Filtered water	Pipe flow	Re: 80,000-105,000 C: 100&200 ppm	70
Mohsenipour et al. [50]	Tab water& Deionized water	Pipelines	Re: 2,000-70,000 C: 100–1000 ppm	75
Li et al. [51]	Water	Pipelines	Re: max 140,000 C: 50–200 ppm	52

The main purpose of present research was to establish the correlation between Darcy friction factor (f) and concentration (C), volume flow rate (Q) and temperature (T) using the response surface methodology (RSM). Also, the other purpose of the current study is to examine the impact of C, T and Q on the drag reduction property of PAM in the turbulent flow regime and also the statistical analysis of the results. Providing an equation to predict the f of polymeric solution and comparing it with other equations in the literature was the other goal of the research.

2. Experiments

2.1. Materials

In this research, distilled water (DW) employed as the base fluid. This research is fundamentally done by measuring the pressure drop before and after dissolving polymer to the pipe under different operating conditions. Table 2 exhibits the specifications of PAM, (supplied by Sigma-Aldrich). PAM, represented by the chemical formula (C_3H_5NO) n, is a water soluble polymer that consists of acrylamide monomers or a combination of acrylamide and acrylic acid monomers. The Mw of commercial PAM varies between 10^5 and 10^7 Da. High Mw PAM (>10^6 Da) has a wider range of usages resultant its high viscosity, drag reduction abilities and water retention properties [2, 52, 53].The drag reduction characteristics of PAM are attributed to the elongation of the polymer, which debilitates the quasi stream wise vortices inherent in turbulent flow [54, 55].

Table 2. Specifications of PAM used in this study

Name (Formula)	Chemical Structure	Mw (Da)	Surface	Moisture	Viscosity (0.5% solution, cP)	Purity	pH value
Polyacrylamide, $(C_3H_5NO)_n$	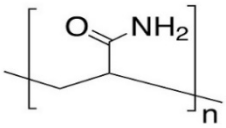	5×10^6	White Finely granule	7.8%	280	99%	6

2.2. Experimental setup and procedure

Utilizing the experimental apparatus employed in our previous studies [5, 39], we investigated the impact of the PAM on pressure drop. Fig. 1 illustrates the schematic of the experimental apparatus.

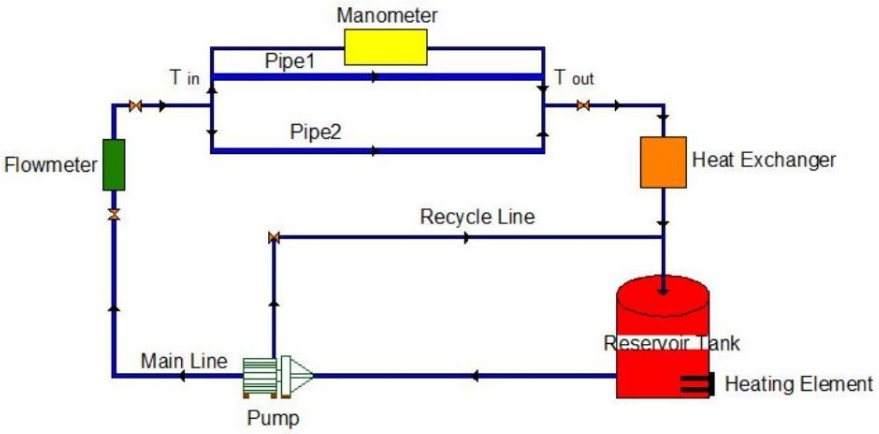

Fig. 1. Schematic of the experimental setup

The diameter and length of the circular pipe (test section) are 0.0127 and 3 *m*, respectively. (The apparatus is equipped with another pipe with a diameter of 0.01905 *m*, which is not used in present study). The test loop contained one reservoir tank, centrifugal pumps, a digital thermostat controller with proportional–integral derivative (PID) controller, metal valves for opening and closing the flow paths, a heater, a U-shaped manometer, flow meters, and a control box. The differential manometer, which possesses an accuracy of ±1 cm-H_2O, measures the variation in fluid height between the two columns of the manometer, thereby indicating the pressure drop across the two ends of the pipe. The pressure drop resulting from the T-junction was determined and subsequently subtracted from the pressure drop indicated by the manometer. To hinder heat loss to the surrounding, the entire system, with particular emphasis

on the pipes, was completely insulated. The output fluid from the test section is cooled to the initial temperature using a heat exchanger before returning to the storage tank. More details and explanations of the experimental set up are given in references [5, 39]. Research assumptions include the following: PAM solution homogeneously distributed in the test section, steady state conditions are established and PAM concentration is assumed to be uniform and constant.

The alterations in viscosity play a crucial role in the investigation of drag reducing polymers (DRP). Consequently, the viscosity of the polymeric solution was measured using an SVM-3000 viscometer from Anton Paar, Austria. Additionally, to achieve more reliable results, the viscosity of distilled water (base fluid) was initially assessed and compared against standard values, yielding an error of approximately ±2.8%, which is considered acceptable.

2.3. Data reduction

The Darcy Weissbach equation shown in Eq. (1) is utilized to specify the experimental friction factor.

$$\mathrm{f} = \frac{2\mathrm{D}}{\rho \mathrm{u}^2}\left(\frac{\Delta \mathrm{P}}{\mathrm{L}}\right) \tag{1}$$

where f is Darcy friction factor, ΔP is the pressure drop of the pipe (Pa), L is the length of the pipe (m), D is the inner diameter of the pipe (m), ρ is the fluid density (kg/m^3), and u is the fluid velocity in the pipe (m/s). The pressure drop resultant the fixed tees at the start and end of the test section, calculated from Eq. (2), is reduced from the pressure drop gained with the differential manometer.

$$h_{f.loss} = k\frac{u^2}{2g} \tag{2}$$

where k is the pressure drop coefficient for T-junction equals to 0.4 [56], and g is the acceleration of gravity (m/s^2). The DRP' effectiveness is defined quantitatively by DR%. DR% was explained as the relative difference between the friction factor of polymeric solution (f_p) and the friction factor of the solvent (f_w), as:

$$DR\% = \left(1 - \frac{f_p}{f_w}\right) \times 100 \tag{3}$$

The impact of friction reduction augments with a rise in polymer concentration, ultimately approaching an asymptotic[1] value. Dissolving further polymer does not influence this value. Virk [2] derived the below equation indicating that the friction reduction is unaffected by the characteristics of the polymer.

$$C_f = 0.58\,\mathrm{Re}^{-0.58} \tag{4}$$

where C_f is Fanning friction factor.

The accuracy of the experimental apparatus was verified by applying distilled water as the working fluid. The outcomes of the tests were compared with the of the Blasius and Colebrook equations [56] thusly:

$$f = \frac{0.316}{\mathrm{Re}^{0.25}} \tag{5}$$

[1] Maximum drag reduction (MDR) asymptote

$$\frac{1}{f^{\frac{1}{2}}} = -2 \times log\left(\frac{2.51}{Re\, f^{\frac{1}{2}}} + \frac{\varepsilon/D}{3.7}\right) \quad (6)$$

where ε describes the carbon steel tube's roughness as 0.05 mm [56].

The range of operational variables and their uncertainties in this study are outlined in Table 3. The uncertainties associated with the variables were determined in accordance with the methodology outlined by Moffat [57]. The maximum uncertainty for the Darcy friction factor was 5.9%. Also, to validate the outcomes of some experiments, they were conducted again, and the repeatability of these outcomes was acceptable.

Table 3. The range of operational parameters and their uncertainty

Parameters	symbol	unit	Range	Uncertainty
Inlet temperature	T	˚C	30-50	±0.1
Flow rate	Q	L/min	6-10	±0.1
Concentration	C	ppm	0-200	0.1%
Reynolds	Re	-	10,200-30,000	2.5%
Pressure drop	ΔP	Pa	8,714-1,951	3.1%
Darcy friction factor	f	-	0.0216-0.0518	5.9%

3. RSM

Response surface methodology (RSM) is a design of experiments (DOE) approach utilized in various engineering applications. It is the method applied to determine the effect of the input parameters on considered responses in association with statistical and mathematical approaches [58-60]. The input parameters are typically designated as independent variables, while the execution scale is referred to as the response [61]. The current study focuses on the development of a regression model for approximation, utilizing empirical data on the friction factor to forecast response variables through RSM, employing Design Expert software version 13.0.0. The capability and reliability of the developed regression model have been examined using the analysis of variance (ANOVA) statistical method. The sum of squares pertains to the source of variance. The degrees of freedom are the sum of the levels considered in the test minus one. The ratio between sum of square values of every factor and its respective degrees of freedom is regarded as mean square. The F ratio is identified as the ratio between the mean square of each factor and the mean square of the residual. The ANOVA approach was employed to evaluate key components, including the coefficient of variation (R-square), Fisher's test (F test), and probability values (P value). These variables are crucial for predicting the suitability of the models developed through regression analysis.

4. Results and discussion

4.1. Validation of the experimental setup

To verify the accuracy of the results of the experimental apparatus, the outcomes of the friction factor calculation are compared with the outcomes of the famous equations. Outcomes demonstrated there was an satisfactory consistency between the experimental findings and calculating the Blasius and Colebrook [56] equations with AARD[2]% of 16%, and 12%, respectively. The results indicate a satisfactory agreement between the experimental outcomes and the theoretical predictions, thereby confirming the validity of the outcomes obtained in this research.

4.2 Statistical analysis

[2] Average Absolute Relative Deviation (AARD)

Data were collected from 27 experimental tests. In the modeling process, three factors influencing the Darcy friction factor (*f*) were identified: concentration (*C*), temperature (*T*), and flow rate (*Q*). The aim of the research is to obtain a relationship to forecast the friction factor of the PAM as drag reducing agent. Therefore, there is a response variable here that is *f*. Various models are analyzed to identify the best one. Table 4 offers additional details regarding the response variable.

Table 4. Response characteristics in friction factor modeling

Response	Name	Units	Observations	Minimum	Maximum	Mean	Std. Dev.	Ratio	Transform
R1	f	-	27.00	0.0216025	0.0518749	0.0350	0.0075	2.40	None

Table 5 presents the p-values, Adjusted R^2, and Predicted R^2 values for the linear model, two-factor interaction (2FI) model, as well as the quadratic and cubic models that were evaluated in the analysis.

Table 5. Summary of statistics for the various models

Source	Sequential p-value	Adjusted R^2	Predicted R^2	
Linear	< 0.0001	0.8886	0.8672	
2FI	0.6640	0.8814	0.8526	
Quadratic	< 0.0001	0.9780	0.9594	Suggested
Cubic	0.3917	0.9696	0.9361	Aliased

The sequential p-value column denotes the importance level of each model term as they were sequentially added to the model. It quantifies the probability of achieving the recorded data or even more extreme results under the assumption that the null hypothesis holds true. A p-value less 0.05 demonstrates that the term is statistically significant, indicating its influence on the variability of the response variable [62]. The adjusted R^2 value reflects the proportion of the overall variance in the dependent variable that is described by the model, while also considering the quantity of independent variables included. An increased adjusted R^2 value implies a better fit between the model and the data. The predicted R^2 column indicates the expected proportion of variability in future observations that the model is capable of explaining. A higher predicted R^2 value implies that the model is anticipated to exhibit strong performance when utilized with new data. From this table, we can see that the quadratic model has the best adjusted R^2 (0.9780) and predicted R^2 (0.9594), which displays that it is the most accurate model to supply the best fit to the data and to forecast the response variable. Table 6 presents the findings of the ANOVA analysis conducted for the quadratic model. Mentioned table is associated to the significance of each parameter.

Table 6. ANOVA outcome for the suggested quadratic model

Source	Sum of Squares	df	Mean Square	F-value	p-value	
Model	0.0015	9	0.0002	129.66	< 0.0001	significant
A-C	0.0006	1	0.0006	468.23	< 0.0001	
B-Q	0.0001	1	0.0001	67.96	< 0.0001	
C-T	0.0007	1	0.0007	538.69	< 0.0001	
AB	9.955E-07	1	9.955E-07	0.8005	0.3834	
AC	4.448E-06	1	4.448E-06	3.58	0.0758	
BC	5.323E-06	1	5.323E-06	4.28	0.0541	
A^2	0.0001	1	0.0001	57.15	< 0.0001	
B^2	1.207E-07	1	1.207E-07	0.0971	0.7591	
C^2	0.0000	1	0.0000	33.76	< 0.0001	
Residual	0.0000	17	1.244E-06			
Cor Total	0.0015	26				

The importance of the modeling is evident from the substantial value of F, which stands at 129.66. P-values symbolize the statistical aspect of the model, and where values are less than 0.05 implies the significance of this parameter, and

parameters with P-values greater than 0.1 have little significance. Consequently, it is possible to eliminate the insignificant components of the model.

Table 7 displays the fit statistics for the quadratic model. The table denotes that the Predicted R^2 value of 0.9594 nearly matches the adjusted R^2 value of 0.9780, with a difference of less than 0.019. This indicates that the model can be trusted upon for predicting future observations. The adeq precision assesses the model's quality by comparing the variation present in the data with the variation anticipated by the model. A ratio exceeding 4 is deemed acceptable, and the calculated ratio of 41.1305 suggests that the model is suitable for investigating the design space.

Table 7. Fit statistics for the quadratic model

Std. Dev.	Mean	CV %	R^2	Adjusted R^2	Predicted R^2	Adeq Precision
0.0011	0.0350	3.18	0.9856	0.9780	0.9594	41.1305

Incorporating the experimental data into the RSM processing model allows for the derivation of an equation as presented in Eq. (7).

$$f = -0.025608 - 0.000102C - 0.000160Q + 0.003060T - 1.51521\times10^{-6}CQ - 6.40540\times10^{-7}CT$$
$$-0.000033QT + 3.82587\times10^{-7}C^2 + 0.000035Q^2 - 0.000026T^2 \quad (7)$$

The equation, represented in terms of its actual factors, can be employed to forecast the response at specified levels of each factor. The original units for each factor should be specified at the levels. This equation should not be utilized to determine the relative influence of each factor. The influence of C, T and Q on friction factor of PAM drag reducing agent is illustrated in Fig. 2. This plot, which is a perturbation in terms of the mentioned factors, displays that the Q has the least impact on f, while the other two parameters had further effect. The mentioned outcomes are in agreement with the results of Raei [39] who reported that the C has the largest contribution in DR of PAN in circular pipes and the contribution of Q and T factors is less.

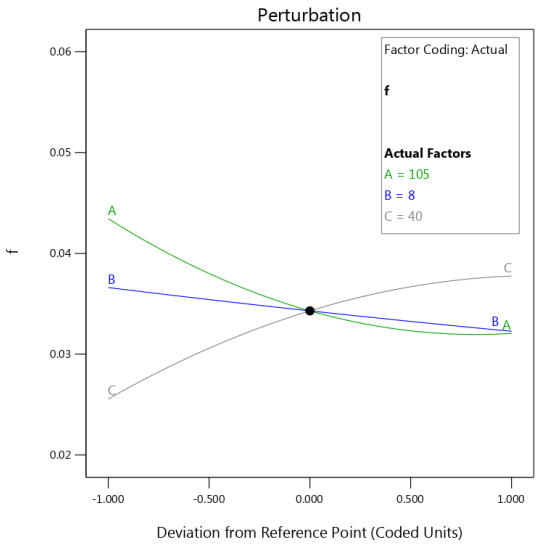

Fig. 2. Perturbation curve for effective factors

The consistency of the results derived from the established relationship for f, in conjunction with the experimental data obtained, is illustrated in Fig. 3. The low deviation of the data from the bisector shows that the experimental data and the acquired data from the suggested correlation are placed next to each other with a satisfactory difference, which shows the high accuracy of the correlation.

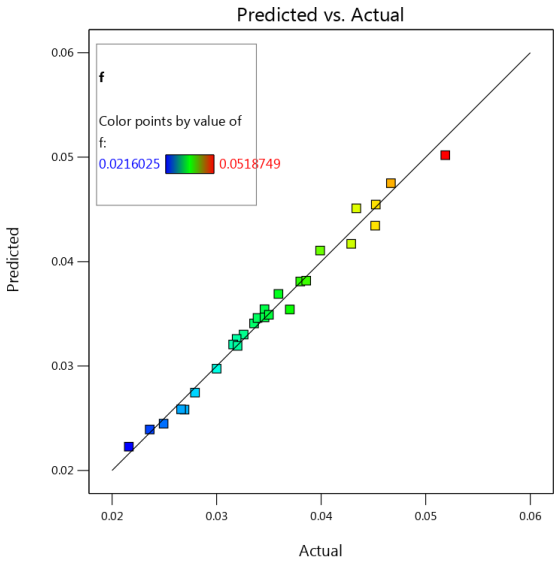

Fig. 3. Comparison of predicted and actual values

In a normal probability plot of residuals (Fig. 4), the alignment of data points along a straight line indicates that the residuals follow a normal distribution. If the data points create an S-shaped curve, it indicates that the data does not follow a normal distribution, necessitating a modification of the mathematical model. The normal probability plots of the experimental data reveal that the residuals are symmetrically distributed around the straight line, with the data points closely aligning with the line. This observation suggests that the residuals of the experimental data conform to the assumption of a normal distribution.

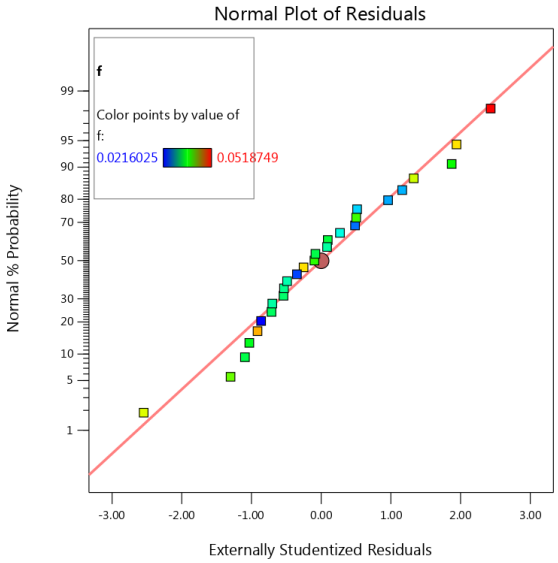

Fig. 4. Normal distribution curve versus residual values

The evaluation of the assumption of constant variance can be conducted by examining the relationship between the predicted values and the residuals. The assumption of constant variance in variance analysis is upheld when the residuals are limited to a specific range. Conversely, if the residuals exhibit an increase with the increase of the predicted values, this assumption is violated, necessitating modifications to the model. The analysis of the friction factor residuals and predicted coefficients presented in Fig. 5 indicates that the experimental residuals are uniformly distributed within the range of ± 3.72. Furthermore, there is no observable trend of divergence in the variance of the

experimental values as the predicted values increase. So, the experimental values satisfy the assumption of constant variance.

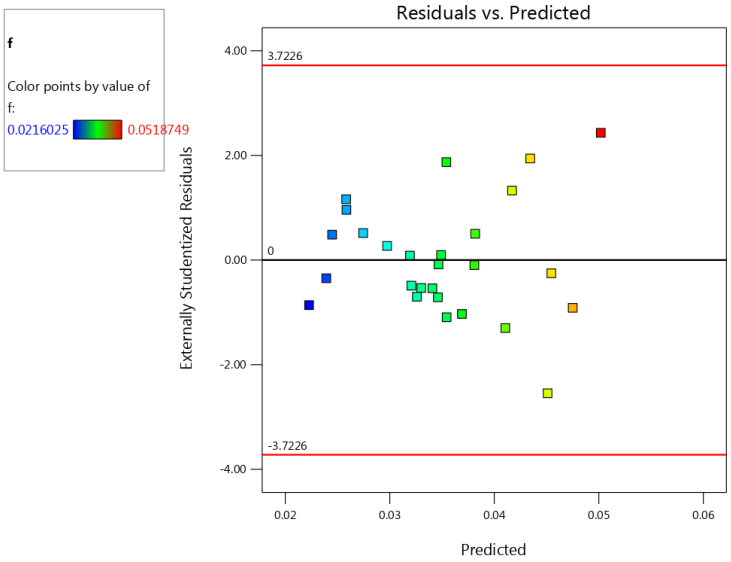

Fig. 5. Curve of predicted and remaining values

The randomness hypothesis may be evaluated by analyzing the relationship between the sequence of runs and the residuals. If there is an obvious time-related trend in the relationship between the sequence of runs and the residuals, it shows that the response includes time-related variables, and the experimental design requires to be modified; otherwise, the data is randomly distributed. Fig 6 illustrates that the residual data falls within the range of ± 3.72, indicating a clear randomness in the relationship between the running time and the residual data. So, the variables are not influenced by time elements and meet with the randomness hypothesis.

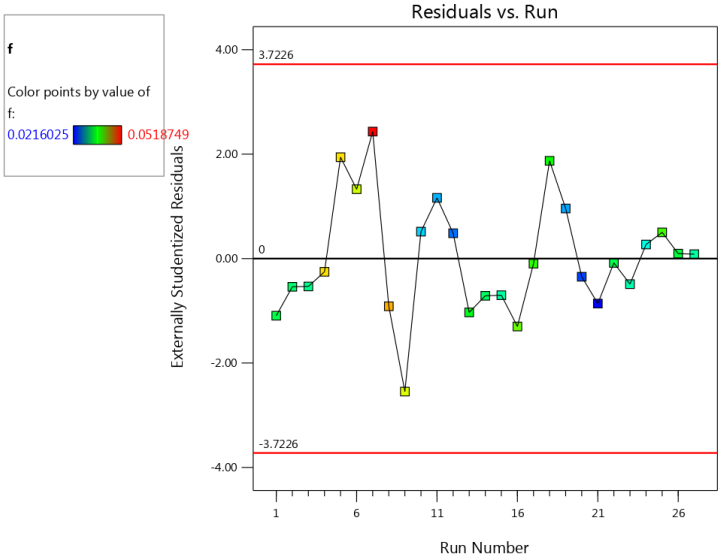

Fig 6. Run number versus residuals

4.2. Impact of the factors and interactions

Factors A and B interact when changes in level A change the effect of B and vice versa. The total number of interactions is $n(n\text{-}1)/2$ for "n" control factors in a design of experiment (DOE). Here, three interactions are caused by three control factors. The criterions for the significance of an interaction are known as P-value and F-value for

understanding the effect of two individual factors at different interaction levels. According to Table 6 (ANOVA), *T* and *Q* possess the highest F-value (4.28), which is equivalent to having the most interaction. Also, to show results visually to examine the simultaneous influence of two parameters on the friction factor, the *f* curves versus *Q* and *C*, the *f* versus *C* and *T* and *f* versus *Q* and *T* are displayed in Fig. 7(a, b, c).

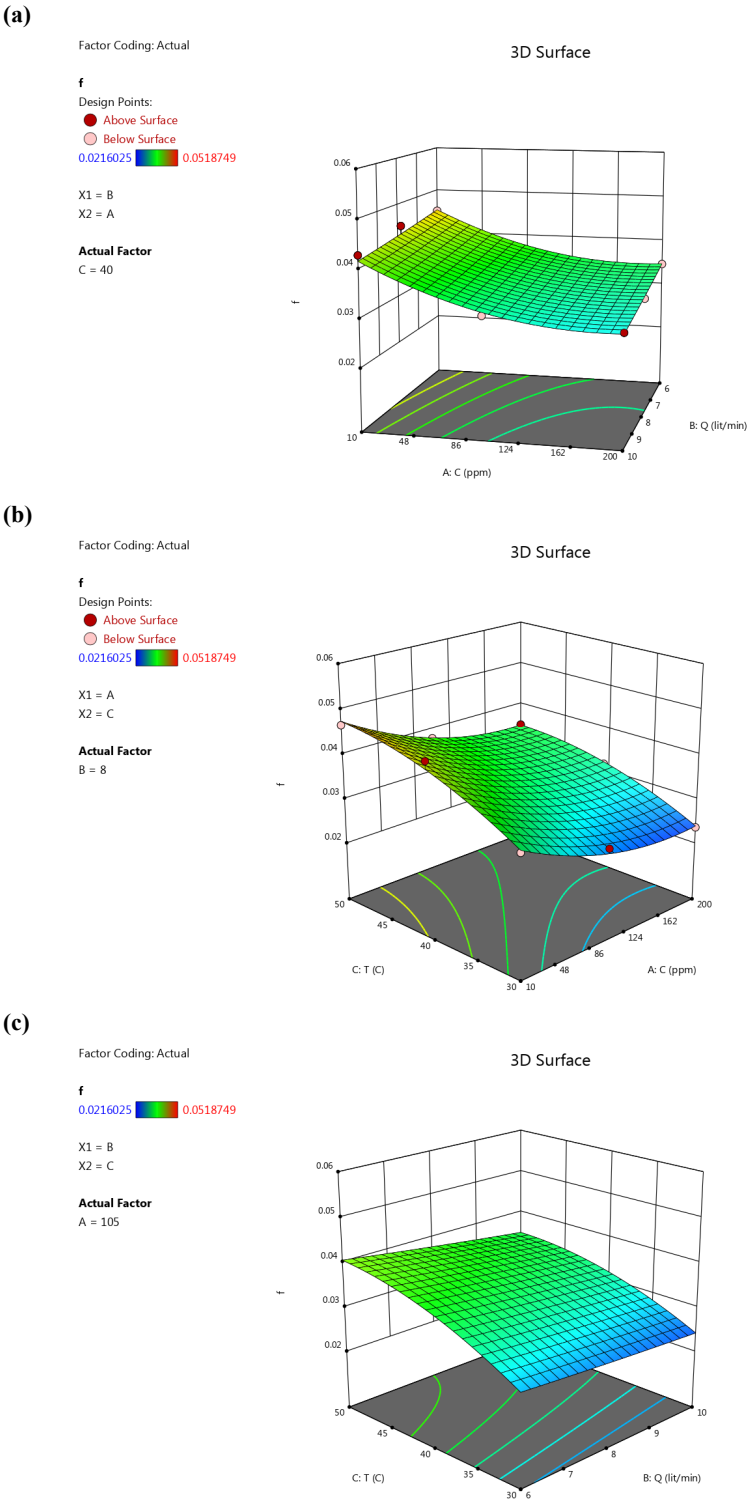

Fig. 7. The effect of different parameters on friction factor; (a) *f* versus *Q* and *C*; (b) *f* versus *C* and T; (c) *f* versus *Q* and *T*

This figure clearly illustrates that the value of *f* experiences a substantial decrease as the concentration increases. Furthermore, changes in *Q* had little impact on *f*. The mentioned results are in agreement with the results of [39].

4.3. Optimum response

Optimization was done on the friction factor of the PAM drag reducer agent to achieve a minimum value. This optimization involved adjusting the *C*, *Q* and *T* of the polymeric solution. In order to optimize the process, the *f* of the polymeric solution was minimized by applying the correlation developed through RSM. The configurations outlined in Table 8 were utilized for this purpose. Results displays the optimum points for the *f*, according to which the *f* of 0.022 in the C=182.111 ppm, T=30 ˚C and Q=10 L/min is optimum. Fig. 8(a,b) illustrates the optimal values for different *C* and *T*. The figure illustrates that the highest level of desirability is observed at more concentrations.

Table 8. Related parameters to optimization of friction factor

Name	Goal	Lower limit	Upper limit	Lower weight	Upper weight	Importance
A:C	is in range	10	200	1	1	3
B:Q	is in range	6	10	1	1	3
C:T	is in range	30	50	1	1	3
f	minimize	0.0216025	0.0518749	1	1	3

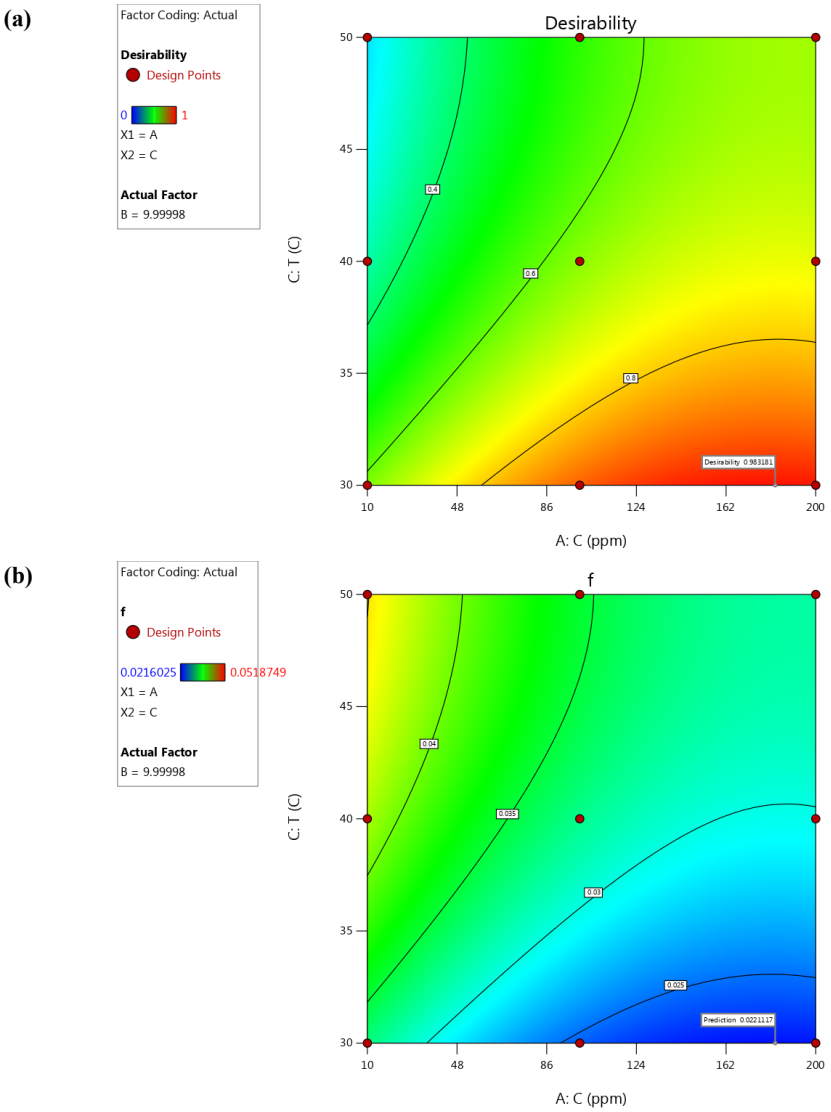

Fig. 8. Optimal values of friction factor in different concentrations (a) desirability (b) *f*

4.4. Modified model

In RSM, ANOVA is typically conducted to determine the P-value associated with each factor. If the P-value is below 0.05, suggesting that the factor's effect on the response variable is important, it can be regarded as a significant factor. If the P-value is greater than 0.1, it suggests that the influence of the factor on the response variable is not statistically important and can be considered disregarded. Eq. (7) takes into account all actual factors and is lengthy and complicated. Numerous factors presented in ANOVA Table 6 exhibit P values exceeding 0.1, suggesting that these factors lack significance and can therefore excluded from the ANOVA table to simplify the model. Following this simplification, the ANOVA table is displayed in Table 9. The simplified correlation is presented in Eq. (8).

$$f = -0.013227 - 0.000140C - 0.001081Q + 0.002727T + 3.82587\times10^{-7}C^2 - 0.000026\times T^2 \quad (8)$$

Table 9. ANOVA outcome for modified model

Source	Sum of Squares	df	Mean Square	F-value	p-value	
Model	0.0014	5	0.0003	188.88	< 0.0001	significant
A-C	0.0006	1	0.0006	381.80	< 0.0001	
B-Q	0.0001	1	0.0001	55.18	< 0.0001	
C-T	0.0007	1	0.0007	440.99	< 0.0001	
A^2	0.0001	1	0.0001	46.60	< 0.0001	
C^2	0.0000	1	0.0000	27.53	< 0.0001	
Residual	0.0000	21	1.525E-06			
Cor Total	0.0015	26				

4.5. Comparison of models

Very limited studies have been done to provide equations for predicting of friction factor of drag reducing agents. We can refer to Ozbayoglu & Ercan [63] and Ozmen & Boersma [37] equations. Fig. 9 shows the ability of Ozbayoglu & Ercan [63] and Ozmen & Boersma [37] equations as well as the RSM model (proposed in the present study) to predict the friction factor of the drag reducing agent. As it is clear from the Fig. 9, the RSM model has been able to perform the prediction with a very good accuracy, but the other two equations do not have such ability.

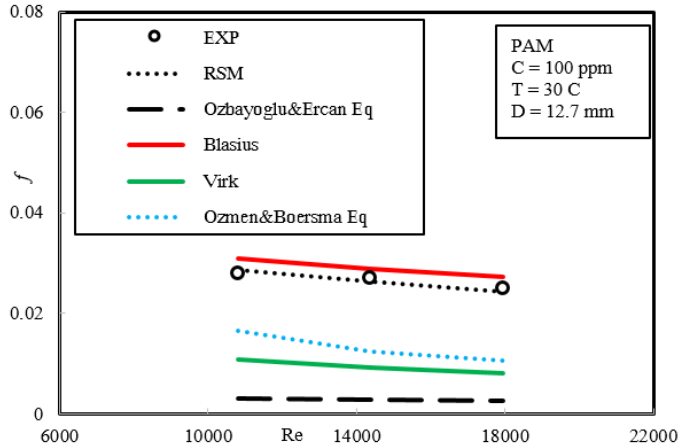

Fig. 9. Comparison of different models in predicting of friction factor

Table 10 shows the accuracy of the three mentioned equations in predicting the friction factor, with different scales. The Average Absolute Relative Deviation (AARD%) in prediction for RSM, Ozbayoglu & Ercan [63],and Ozmen & Boersma [37] equations was 2.4, 89.6, and 50.9%, respectively. In addition, the prediction of friction factor by Ozbayoglu & Ercan [63] equation is lower than the asymptotic value of Virk's [2] equation, which is in contradiction with Virk's [2] results.

Table 10. The comparison between the results of the RSM model and other models for prediction of friction factor

Model	AARD%	MSE[3]	RMSE[4]	Maximum MOD[5]%
RSM (present study)	2.4	4.04×10^{-7}	0.000636	2.9
Ozbayoglu&Ercan [63]	89.6	0.154	0.392	90
Ozmen&Boersma [37]	50.9	0.000183	0.0135	58

5. Conclusion

In this research, we studied experimentally and statistically the drag reduction property of PAM inside the horizontal smooth circular pipe under turbulent flow regime using response surface methodology (RSM). RSM was effectively utilized in this study, yielding equations that accurately predict the friction factor of the PAM. RSM provided different equations to calculate friction factor based on independent parameters such as *C*, *T* and *Q*. The quadratic model has been demonstrated to be superior to the other models through the use of statistical parameters and plots. R^2, adjusted R^2, predicted R^2 and Std. Dev parameters of the quadratic model were equal to 0.9856, 0.9780, 0.9594 and 0.0011 respectively, which signifies the accuracy of the model. As well, the difference between adjusted R^2 and predicted R^2 is less than 0.019 indicates the high accuracy of the proposed model. The residual plot, the normal probability plot and the predicted vs. actual plot also showed that quadratic model has a good accuracy, and is well capable of predicting friction factor of the PAM. The experimental outcomes displayed that with increasing *C*, the friction factor decreases intensely but, changes in *Q* had little effect on friction factor. This trend was predicted by RSM methods with very high accuracy. The optimum combination for better friction factor was found at C = 182.111 ppm, T = 45 °C and Q = 10 L/min.

Nomenclature

Symbols

C	Concentration
C_f	Fanning friction factor
Da	Dalton
f	Darcy friction factor
g	Gravitational acceleration
gr	gram
hp	horsepower
l	Litter
k	Coefficient for T-junction
L	Tube Length
M	Molecular weight
P	Pressure
Q	Volume flow rate
T	Temperature
u	Velocity

Greek symbols

ε	Roughness
μ	Viscosity
ρ	Density

Subscripts

Exp	experimental

Abbreviation

CMC	Carboxymethyl cellulose
DOE	Design of experiment
DR	Drag reduction
DRAs	Drag reducing agents
DRPs	Drag reducing polymers
DW	Deionised water
GG	Guar Gum
MDR	Maximum drag reduction
ppm	Parts per million
PAA	Polyacrylic acid
PAM	Polyacrylamide
PAN	Polyacrylonitrile
PEO	Polyethylene oxide
PID	Proportional–integral derivative
XG	Xanthan Gum

References

[1] Toms, B.A., 1948. Some observation on the flow of linear polymer solution Through straight tubes at large Reynolds number, paper presented at Proceeding of the First International Congress on Rheology, North Holland, Amsterdam.
[2] Virk, P.S., 1975. Drag reduction fundamentals. AIChE Journal, 21(4), 625-656. https://doi.org/10.1002/aic.690210402
[3] Den Toonder, J., Draad, A., Kuiken, G., Nieuwstadt, F., 1995. Degradation effects of dilute polymer solutions on turbulent drag reduction in pipe flows. Applied Scientific Research, 55(1), 63-82. https://doi.org/10.1007/BF00854224

[3] Mean square error
[4] Root mean square error
[5] Margin of deviation

[4] Kim, N.-J., Kim, S., Lim, S.H., Chen, K., Chun, W., 2009. Measurement of drag reduction in polymer added turbulent flow. international communications in heat and mass transfer, 36(10), 1014-1019. http://dx.doi.org/10.1016/j.icheatmasstransfer.2009.08.002
[5] Raei, B., Peyghambarzadeh, S.M., 2021. Experimental Investigation of Drag Reduction in Turbulent Flow Using Biological and Synthetic Macromolecules: A Comparative Study. Journal of Chemical and Petroleum engineering, 55(1), 117-137. http://dx.doi.org/10.22059/jchpe.2021.307767.1323
[6] Sung, J., Kim, C., Choi, H., Hur, B., Kim, J., Jhon, M., 2004. Turbulent drag reduction efficiency and mechanical degradation of poly (acrylamide). Journal of Macromolecular Science, Part B, 43(2), 507-518. https://doi.org/10.1081/MB-120029784
[7] Chen, Y., Niu, P., He, M., Li, C., Nechval, A.M., Valeev, A.R., Yang, P., 2025. Turbulent drag reduction behavior of polymer solutions in different geometries. Energy, 323, 135798. https://doi.org/10.1016/j.energy.2025.135798
[8] Chen, Y., Lin, X., He, M., Yang, P., Li, C., Nechval, A.M., Valeev, A.R., 2025. An experimental investigation on the turbulent drag reduction effect of polyacrylamide solution in the loop pipe. Journal of Pipeline Science and Engineering, 100264. https://doi.org/10.1016/j.jpse.2025.100264
[9] Xu, J., Zhou, N., Zhang, J., Yao, Y., Wang, H., Liu, S., 2025. Study on rheological properties of large particle gangue slurry and its drag reduction effect caused by wall slippage in pipeline transportation. Powder Technology, 452, 120573. https://doi.org/10.1016/j.powtec.2024.120573
[10] Barbosa, K.C.O., Soares, E.J., Khalil, M.C., Karnitz, O., 2025. Polymer drag reduction in dispersed oil–water flow in tubes. International Journal of Multiphase Flow, 183, 105064. https://doi.org/10.1016/j.ijmultiphaseflow.2024.105064
[11] Zhou, Z., Li, M., Ge, Z., Zhang, X., Tang, Y., Cui, J., Gong, S., 2025. Drag reduction characteristics of RJD-suitable surfactant-polymer composite fluids under high shear. international communications in heat and mass transfer, 160, 108341. https://doi.org/10.1016/j.icheatmasstransfer.2024.108341
[12] Shi, P.-f., Hu, H.-b., Wen, J., Xie, L., 2024. Drag reduction and degradation of binary polymer solutions. Journal of non-newtonian fluid mechanics, 105279. https://doi.org/10.1016/j.jnnfm.2024.105279
[13] Brandfellner, L., Muratspahić, E., Bismarck, A., Müller, H.W., 2024. Quantitative description of polymer drag reduction: Effect of polyacrylamide molecular weight distributions. Journal of non-newtonian fluid mechanics, 325, 105185. https://doi.org/10.1016/j.jnnfm.2024.105185
[14] Cheng, Z., Zhang, P., Wang, X., Song, X., Dai, X., Gao, L., Zhang, X., Zhang, G., Lu, Y., 2024. Drag reduction and degradation by sodium alginate in turbulent flow. Scientific Reports, 14(1), 16854. https://doi.org/10.1038/s41598-024-67873-2
[15] Pereira, A.S., Andrade, R.M., Soares, E.J., 2013. Drag reduction induced by flexible and rigid molecules in a turbulent flow into a rotating cylindrical double gap device: Comparison between Poly (ethylene oxide), Polyacrylamide, and Xanthan Gum. Journal of non-newtonian fluid mechanics, 202, 72-87. https://doi.org/10.1016/j.jnnfm.2013.09.008
[16] Sandoval, G.A., Soares, E.J., 2016. Effect of combined polymers on the loss of efficiency caused by mechanical degradation in drag reducing flows through straight tubes. Rheologica Acta, 55(7), 559-569. https://doi.org/10.1007/s00397-016-0927-6
[17] Sitaramaiah, G., Smith, C.L., 1969. Turbulent drag reduction by polyacrylamide and other polymers. Society of Petroleum Engineers Journal, 9(02), 183-188. https://doi.org/10.2118/2405-PA
[18] Jouenne, S., Anfray, J., Cordelier, P.R., Mateen, K., Levitt, D., Souilem, I., Marchal, P., Lemaitre, C., Choplin, L., Nesvik, J., Waldman, T., 2015. Degradation (or lack thereof) and drag reduction of HPAM solutions during transport in turbulent flow in pipelines. Oil and gas facilities, 4(01), 80-92. https://doi.org/10.2118/169699-PA
[19] Raei, B., Shahraki, F., Peyghambarzadeh, S.M., 2018. Experimental study of the effect of drag reducing agent on heat transfer and pressure drop characteristics. Experimental Heat Transfer, 31(1), 68-84. https://doi.org/10.1080/08916152.2017.1353557
[20] Graham, M.D., 2004. Drag reduction in turbulent flow of polymer solutions. Rheology reviews, 2(2), 143-170.
[21] Tiong, A.N.T., Kumar, P., Saptoro, A., 2015. Reviews on drag reducing polymers. Korean Journal of Chemical Engineering, 32, 1455-1476. https://doi.org/10.1007/s11814-015-0104-0
[22] Abubakar, A., Al-Wahaibi, T., Al-Wahaibi, Y., Al-Hashmi, A., Al-Ajmi, A., 2014. Roles of drag reducing polymers in single-and multi-phase flows. Chemical Engineering Research and Design, 92(11), 2153-2181. https://doi.org/10.1016/j.cherd.2014.02.031
[23] Brostow, W., 2008. Drag reduction in flow: Review of applications, mechanism and prediction. Journal of Industrial and Engineering Chemistry, 14(4), 409-416. https://doi.org/10.1016/j.jiec.2008.07.001
[24] Asidin, M., Suali, E., Jusnukin, T., Lahin, F., 2019. Review on the applications and developments of drag reducing polymer in turbulent pipe flow. Chinese Journal of Chemical Engineering, 27(8), 1921-1932. https://doi.org/10.1016/j.cjche.2019.03.003
[25] Han, W.J., Dong, Y.Z., Choi, H.J., 2017. Applications of water-soluble polymers in turbulent drag reduction. Processes, 5(2), 24. https://doi.org/10.3390/pr5020024
[26] Rushd, S., Ferroudji, H., Yousuf, H., Walker, T.W., Basu, A., Sen, T.K., 2024. Applications of drag reducers for the pipeline transportation of heavy crude oils: A critical review and future research directions. The Canadian Journal of Chemical Engineering, 102(1), 438-458. https://doi.org/10.1002/cjce.25023
[27] Soares, E.J., 2020. Review of mechanical degradation and de-aggregation of drag reducing polymers in turbulent flows. Journal of non-newtonian fluid mechanics, 276, 104225. https://doi.org/10.1016/j.jnnfm.2019.104225
[28] Zhang, K., Lim, G.H., Choi, H.J., 2016. Mechanical degradation of water-soluble acrylamide copolymer under a turbulent flow: Effect of molecular weight and temperature. Journal of Industrial and Engineering Chemistry, 33, 156-161. https://doi.org/10.1016/j.jiec.2015.09.031

[29] Zhang, X., Duan, X., Muzychka, Y., 2018. New mechanism and correlation for degradation of drag-reducing agents in turbulent flow with measured data from a double-gap rheometer. Colloid and Polymer Science, 296(4), 829-834. https://doi.org/10.1007/s00396-018-4300-4
[30] Brostow, W., 1983. Drag reduction and mechanical degradation in polymer solutions in flow. Polymer, 24(5), 631-638. https://doi.org/10.1016/0032-3861(83)90119-2
[31] Habibpour, M., Clark, P.E., 2017. Drag reduction behavior of hydrolyzed polyacrylamide/xanthan gum mixed polymer solutions. Petroleum Science, 14(2), 412-423. https://doi.org/10.1007/s12182-017-0152-7
[32] Choi, H.J., Kim, C.A., Sohn, J.-I., Jhon, M.S., 2000. An exponential decay function for polymer degradation in turbulent drag reduction. Polymer Degradation and Stability, 69(3), 341-346. https://doi.org/10.1016/S0141-3910(00)00080-X
[33] Karami, H.R., Rahimi, M., Ovaysi, S., 2018. Degradation of drag reducing polymers in aqueous solutions. Korean Journal of Chemical Engineering, 35(1), 34-43. https://doi.org/10.1007/s11814-017-0264-1
[34] Virk, P., Sherman, D., Wagger, D., 1997. Additive equivalence during turbulent drag reduction. American Institute of Chemical Engineers. AIChE Journal, 43(12), 3257.
[35] Lumley, J.L., 1977. Drag reduction in two phase and polymer flows. Physics of Fluids (1958-1988), 20(10), S64-S71. https://doi.org/10.1063/1.861760.
[36] Tulin, M.P., 1967. Hydrodynamic aspects of macromolecular solutions. Technical Report 353-4, Hydronautics Incorporated, Research in Hydrodynamics, Washington DC, USA.
[37] Ozmen, Y., Boersma, B.J., 2023. An experimental study on friction reducing polymers in turbulent pipe flow. Ocean Engineering, 274, 114039. https://doi.org/10.1016/j.oceaneng.2023.114039
[38] Cheng, Z., Zhang, X., Song, X., Wang, X., Zhang, G., Lu, Y., Li, L., Liu, F., Dai, X., 2023. Investigation of drag reduction by slurry-like drag-reducing agent in microtube flow using response surface methodology (RSM). Scientific Reports, 13(1), 22433. https://doi.org/10.1038/s41598-023-49804-9
[39] Raei, B., 2023. The effect of polymeric drag reducing agent on pressure drop reduction in circular pipes: Experimental and statistical investigation. Journal of the Indian Chemical Society, 100(3), 100905. https://doi.org/10.1016/j.jics.2023.100905
[40] Varnaseri, M., Peyghambarzadeh, S.M., Amiri, M., 2018. Experimental study on optimum concentration of polyacrylamide for drag reduction and heat transfer performance in a compact heat exchanger. Heat and Mass Transfer. https://doi.org/10.1007/s00231-018-02533-6
[41] Sandoval, G., Trevelin, R., Soares, E., Silveira, L., Thomaz, F., Pereira, A., 2018. Polymer degradation in turbulent drag reducing flows in pipes. RETERM-Thermal Engineering, 14(2), 03-06. https://dx.doi.org/10.5380/reterm.v14i2.62123
[42] Lim, S., Choi, H., Lee, S., So, J., Chan, C., 2003. λ-DNA induced turbulent drag reduction and its characteristics. Macromolecules, 36(14), 5348-5354. https://doi.org/10.1021/ma025964k
[43] Liberatore, M.W., Baik, S., McHugh, A.J., Hanratty, T.J., 2004. Turbulent drag reduction of polyacrylamide solutions: effect of degradation on molecular weight distribution. Journal of non-newtonian fluid mechanics, 123(2-3), 175-183. https://doi.org/10.1016/j.jnnfm.2004.08.006
[44] Khadom, A.A., Abdul-Hadi, A.A., 2014. Performance of polyacrylamide as drag reduction polymer of crude petroleum flow. Ain Shams Engineering Journal, 5(3), 861-865. http://dx.doi.org/10.1016/j.asej.2014.04.005
[45] Andrade, R.M., Pereira, A.S., Soares, E.J., 2016. Drag reduction in synthetic seawater by flexible and rigid polymer addition into a rotating cylindrical double gap device. Journal of Fluids Engineering, 138(2), 021101. https://doi.org/10.1115/1.4031229
[46] Varnaseri, M., Peyghambarzadeh, S., 2020. The effect of polyacrylamide drag reducing agent on friction factor and heat transfer coefficient in laminar, transition and turbulent flow regimes in circular pipes with different diameters. International Journal of Heat and Mass Transfer, 154, 119815. https://doi.org/10.1016/j.ijheatmasstransfer.2020.119815
[47] Liu, D., Wang, Q., Wei, J., 2018. Experimental study on drag reduction performance of mixed polymer and surfactant solutions. Chemical Engineering Research and Design, 132, 460-469. https://doi.org/10.1016/j.cherd.2018.01.047
[48] Varnaseri, M., Peyghambarzadeh, S., 2020. Comprehensive Study of the Effect of the Addition of Four Drag Reducing Macromolecules on the Pressure Drop and Heat Transfer Performance of Water in a Finned Tube Heat Exchanger. Journal of Macromolecular Science, Part B, 59(11), 747-773. https://doi.org/10.1080/00222348.2020.1801194
[49] Rho, T., Park, J., Kim, C., Yoon, H.-K., Suh, H.-S., 1996. Degradation of polyacrylamide in dilute solution. Polymer Degradation and Stability, 51(3), 287-293. https://doi.org/10.1016/0141-3910(95)00182-4
[50] Mohsenipour, A.A., Pal, R., Prajapati, K., 2013. Effect of cationic surfactant addition on the drag reduction behaviour of anionic polymer solutions. The Canadian Journal of Chemical Engineering, 91(1), 181-189. https://doi.org/10.1002/cjce.20686
[51] Li, E., Zheng, L., Li, Y., Fan, L., Zhao, S., Liu, S., 2022. Investigation of the drag reduction of hydrolyzed polyacrylamide–xanthan gum composite solution in turbulent flow. Asia-Pacific Journal of Chemical Engineering, 17(5), e2791. https://doi.org/10.1002/apj.2791
[52] Tolstikh, L., Akimov, N., Golubeva, I., Shvetsov, I., 1992. Degradation and stabilization of polyacrylamide in polymer flooding conditions. International Journal of Polymeric Materials, 17(3-4), 177-193. https://doi.org/10.1080/00914039208041113
[53] Xiong, B., Loss, R.D., Shields, D., Pawlik, T., Hochreiter, R., Zydney, A.L., Kumar, M., 2018. Polyacrylamide degradation and its implications in environmental systems. npj Clean Water, 1(1), 17. https://dx.doi.org/10.1038/s41545-018-0016-8
[54] Dubief, Y., Terrapon, V.E., White, C.M., Shaqfeh, E.S., Moin, P., Lele, S.K., 2005. New answers on the interaction between polymers and vortices in turbulent flows. Flow, turbulence and combustion, 74, 311-329. https://doi.org/10.1007/s10494-005-9002-6
[55] White, C.M., Mungal, M.G., 2008. Mechanics and Prediction of Turbulent Drag Reduction with Polymer Additives. Annual review of fluid mechanics, 40(1), 235-256. https://dx.doi.org/10.1146/annurev.fluid.40.111406.102156

[56] White, F.M., 2001. Fluid Mechanics, fourth ed ed, McGraw-Hill, Inc, New York.
[57] Moffat, R.J., 1988. Describing the uncertainties in experimental results. Experimental Thermal and Fluid Science, 1(1), 3-17. http://dx.doi.org/10.1016/0894-1777(88)90043-X
[58] Moraveji, M.K., Razvarz, S., 2012. Experimental investigation of aluminum oxide nanofluid on heat pipe thermal performance. international communications in heat and mass transfer, 39(9), 1444-1448. https://doi.org/10.1016/j.icheatmasstransfer.2012.07.024
[59] Samimi, A., Zakeri, M., Maleki, B., Mohebbi-Kalhori, D., 2015. Experimental and statistical assessments of the mechanical strength reliability of gamma alumina catalyst supports. Particuology, 21, 74-81. https://doi.org/10.1016/j.partic.2014.10.002
[60] Zakeri, M., Moghadam, H., Samimi, A., Mohebbi-Kalhori, D., 2019. Optimization of calcium alginate beads production by electrospray using response surface methodology. Materials Research Express, 6(9), 095412. https://dx.doi.org/10.1088/2053-1591/ab3377
[61] Esfe, M.H., Wongwises, S., Naderi, A., Asadi, A., Safaei, M.R., Rostamian, H., Dahari, M., Karimipour, A., 2015. Thermal conductivity of Cu/TiO2–water/EG hybrid nanofluid: Experimental data and modeling using artificial neural network and correlation. international communications in heat and mass transfer, 66, 100-104. https://doi.org/10.1016/j.icheatmasstransfer.2015.05.014
[62] Lau, H.-L., Wong, F.W.F., Abd Rahman, R.N.Z.R., Mohamed, M.S., Ariff, A.B., Hii, S.-L., 2023. Optimization of fermentation medium components by response surface methodology (RSM) and artificial neural network hybrid with genetic algorithm (ANN-GA) for lipase production by Burkholderia cenocepacia ST8 using used automotive engine oil as substrate. Biocatalysis and Agricultural Biotechnology, 50, 102696. https://doi.org/10.1016/j.bcab.2023.102696
[63] ÖZbayoğlu, M., Ercan, C., 2010. PHPA as a frictional pressure loss reducer and its pressure loss estimation. Petroleum Science and Technology, 28(6), 625-631. https://doi.org/10.1080/10916460903070371